Higgs properties and EFT measurements from ATLAS

Alex Wang

University of California – Santa Cruz

On behalf of the ATLAS experiment

Φαινό 2026

The 2026 Phenomenology Symposium

Introduction (1)

Since its discovery, huge effort to test all Higgs boson properties

Deviations could reveal signs of BSM physics

- Vector boson and fermion couplings: Nature 607 52 (2022)
  - $\kappa_V = 1.04 \pm 0.03, \kappa_F = 0.95 \pm 0.05$
- Higgs mass: Phys. Rev. Lett. 131 (2023) 251802
  - $m_H = 125.11 \pm 0.11$ GeV
- Total width: Phys. Lett. B 846 (2023) 138223
  - $\Gamma_H = 4.4^{+3.0}_{-2.2}$ MeV
- Spin 0: Phys. Lett. B 726 (2013) 120

Today will be about Higgs coupling CP as well as effective field theory (EFT) interpretations

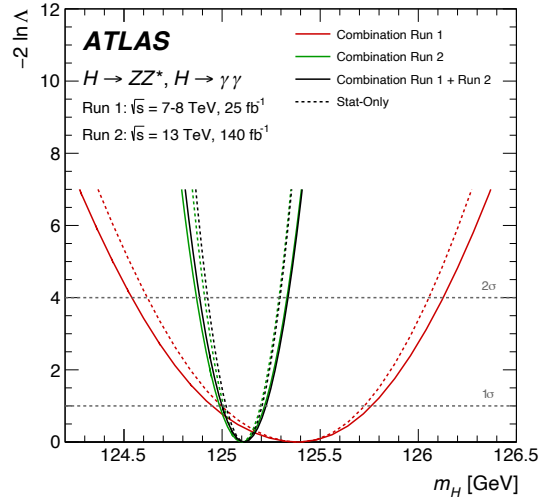

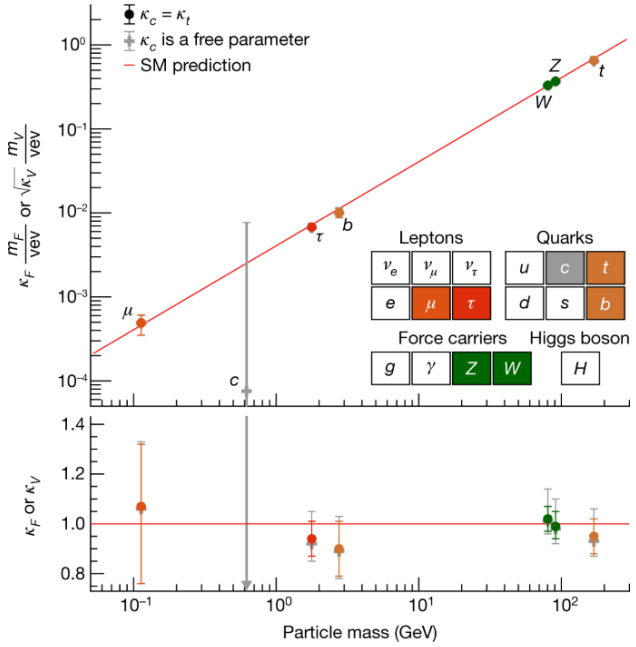

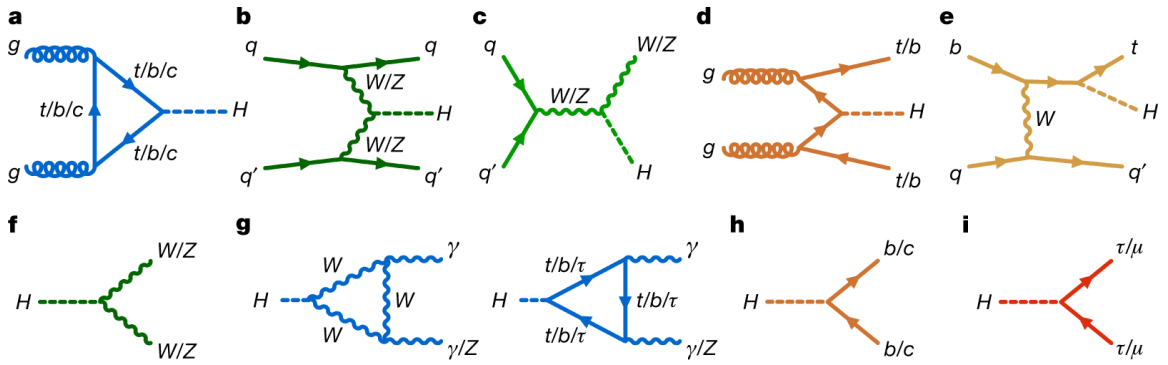

Introduction (2)

BSM effects can be formalized using the Standard Model Effective Field Theory framework as higher order dimensional 6 operators added to the usual SM Lagrangian

$$\mathcal{L}_{\text{SMEFT}} = \mathcal{L}_{\text{SM}} + \sum_i \frac{c_i^{(5)}}{\Lambda} O_i^{(5)} + \sum_i \frac{c_i^{(6)}}{\Lambda^2} O_i^{(6)} + \ldots, \qquad \Lambda = 1 \text{ TeV}$$

Violates lepton and baryon number

$$|\mathcal{M}_{\text{SMEFT}}|^2 = |\mathcal{M}_{\text{SM}}|^2 + 2\sum_i \frac{c_i}{\Lambda^2} \text{Re}(\mathcal{M}_{\text{SM}}^* \mathcal{M}_i) + \sum_{i,j} \frac{c_i c_j}{\Lambda^4} (\mathcal{M}_i^* \mathcal{M}_j),$$

Linear interference

Quadratic (excluding d = 8 contributions)

To test for CP violation, one can construct CP-odd optimal observables (OO) by condensing multi-dimensional phase space information into a single variable

$$OO = \frac{2\Re(\mathcal{M}_{\text{SM}}^* \mathcal{M}_{\text{CP-odd}})}{|\mathcal{M}_{\text{SM}}|^2}.$$

CP invariance ⇒ average over entire phase space <OO> = 0

JHEP 10 (2025) 92

VBF $H \rightarrow \tau\tau$ CP Run 2

Use of high $H \rightarrow \tau\tau$ branching ratio to search for CP violation via CP-odd coefficient $c_{H\tilde{W}}$ in Warsaw basis

Events selected using a separate NN in each tau decay channel, insensitive to CP

$$\frac{c_{H\tilde{W}}}{\Lambda^2} H^\dagger H \tilde{W}^I_{\mu\nu} W^{\mu\nu I}$$

Results obtained using the optimal observable method built from Higgs + VBF jet 4-vectors

Among most stringent Run 2 constraints

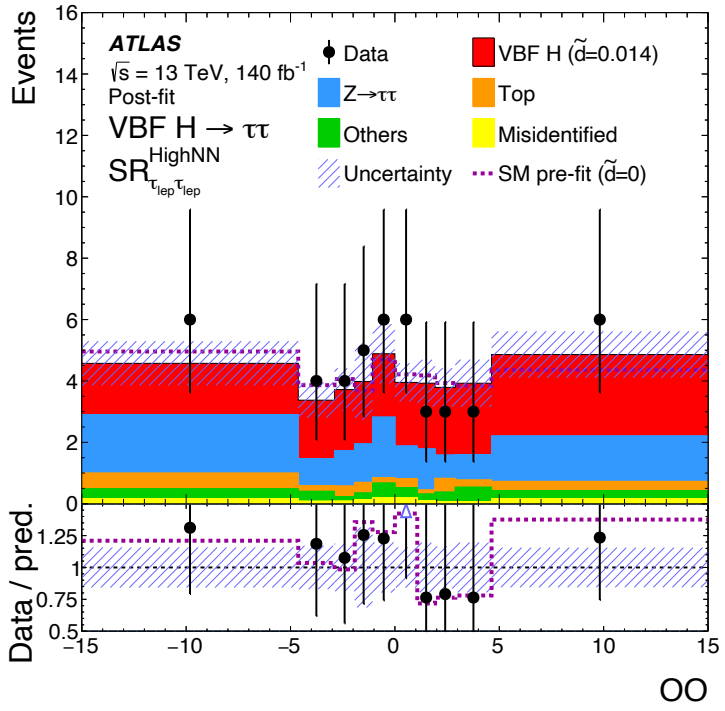

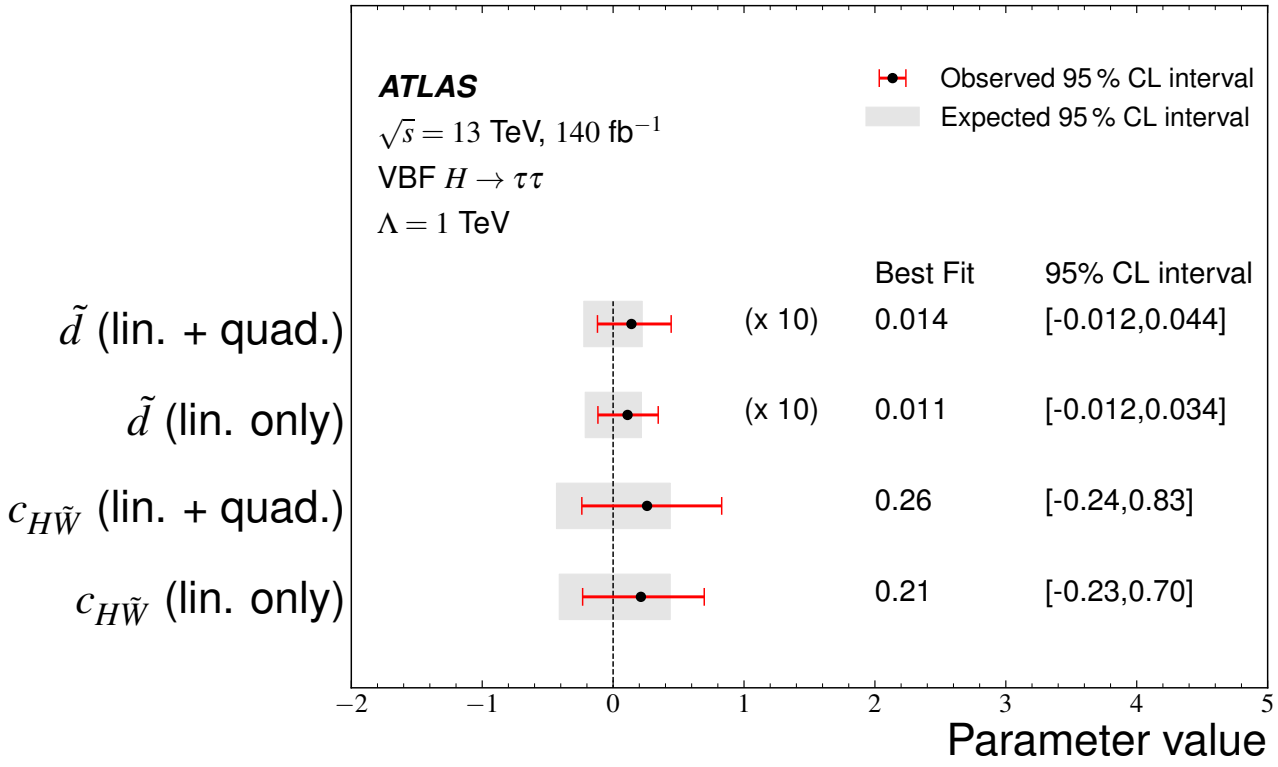

HISZ basis

Warsaw basis

arXiv:2603.20117

HVV CP combination Run 2

HVV CP violation described via 3 CP odd coefficients $c_{H\tilde{W}}, c_{H\tilde{B}}, c_{H\tilde{W}B}$ in the Warsaw basis

$$\frac{c_{H\tilde{W}}}{\Lambda^2} H^\dagger H \tilde{W}^I_{\mu\nu} W^{\mu\nu I}, \frac{c_{H\tilde{B}}}{\Lambda^2} H^\dagger H \tilde{B}_{\mu\nu} B^{\mu\nu}, \frac{c_{H\tilde{W}B}}{\Lambda^2} H^\dagger H \sigma^I \tilde{W}^I_{\mu\nu} B^{\mu\nu},$$

Probed via combination of Run 2 VBF, VH production modes and $H \to ZZ^*, H \to WW^*$ decays

Input analysis	Observable
$H \to ZZ^*$	$OO_{jj}^{c_{H\tilde{W}}}$ (VBF prod), $OO_{4l}^{c_{H\tilde{W}}}, OO_{4l}^{c_{H\tilde{B}}}$, $OO_{4l}^{c_{HW\tilde{B}}}$ (decay)
VBF $H \to \gamma\gamma$	OO_{jj} (prod)
VBF $H \to \tau\tau$	OO_{jj} (prod)
ggF + VBF $H \to WW^*$	STXS + $\Delta\phi_{jj}$
$WH(\to bb)$	STXS + $Q_l cos\delta^+$

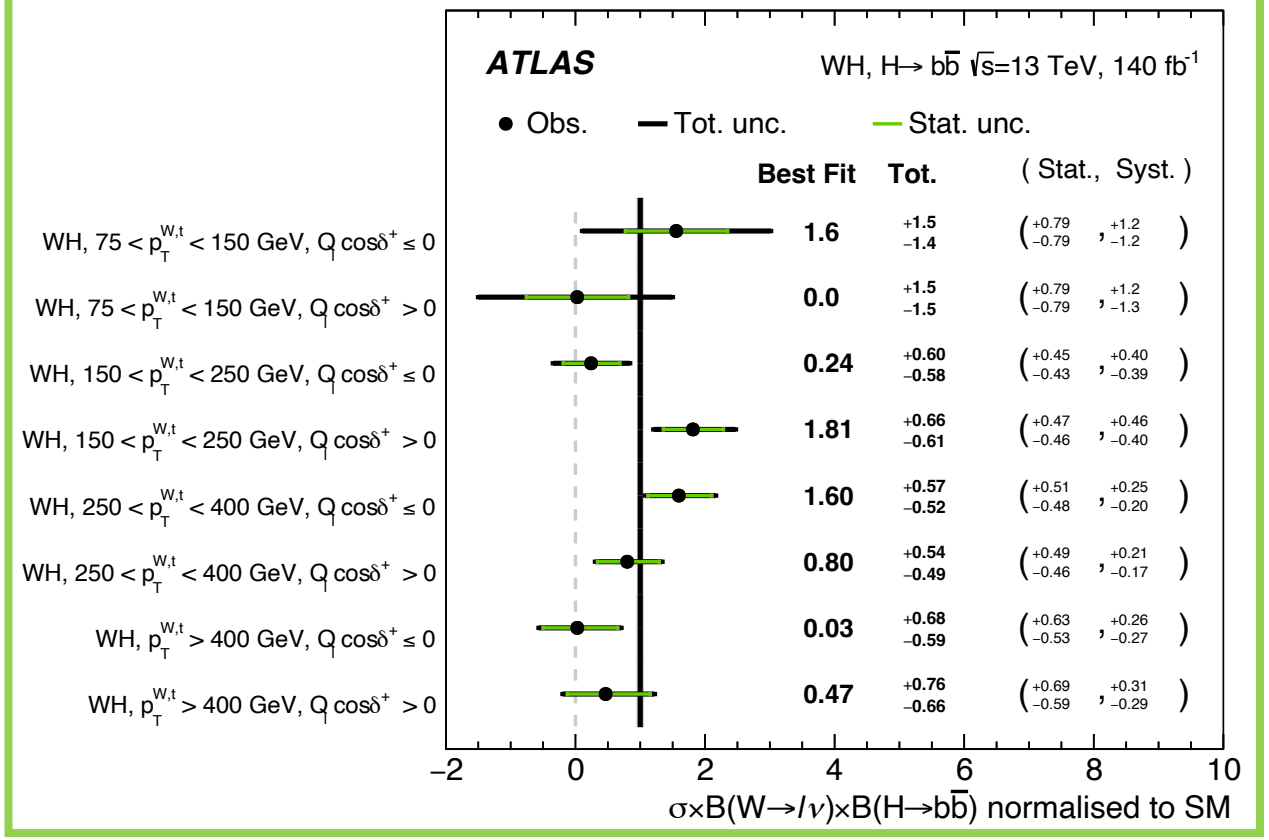

New in this combination!

$$cos\delta^+ = \frac{\mathbf{p}_\ell^{(W)} \cdot (\mathbf{p}_H \times \mathbf{p}_W)}{|\mathbf{p}_\ell^{(W)}| \cdot |\mathbf{p}_H \times \mathbf{p}_W|}$$

arXiv:2603.20117

HVV CP combination Run 2

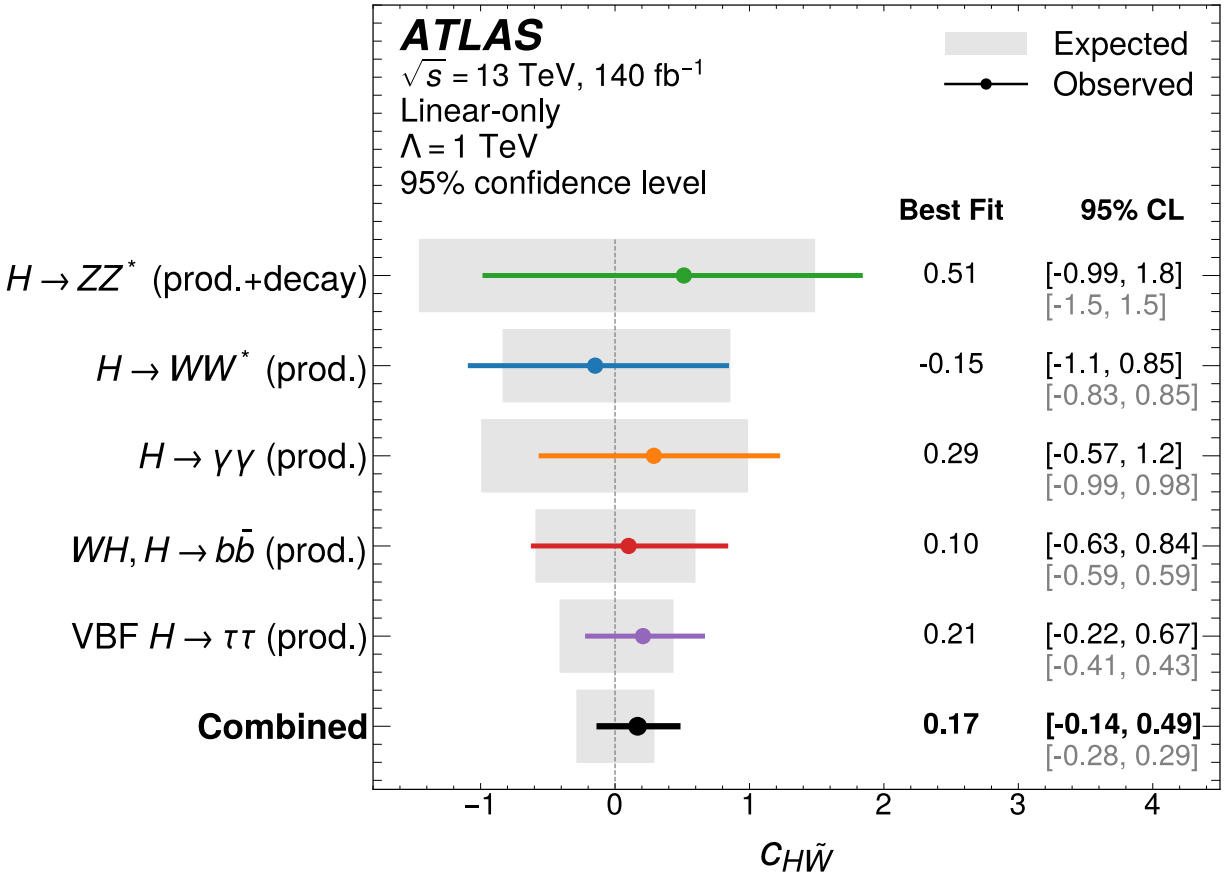

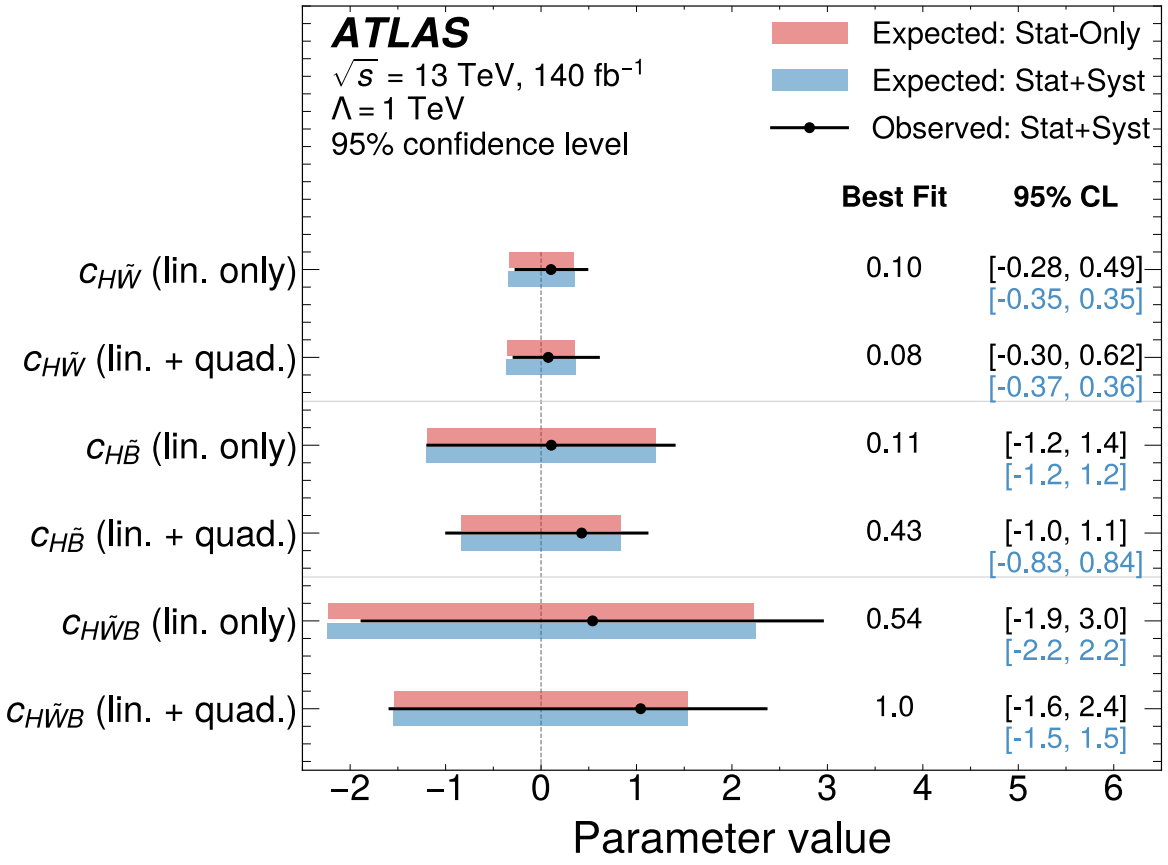

Combination improves over 40% with respect to individual analyses on $c_{H\tilde{W}}$

First time simultaneous constraints on $c_{H\tilde{W}}, c_{H\tilde{B}}, c_{H\tilde{W}B}$ and most stringent to date

VBF $H \to \gamma\gamma$ CP Run 3

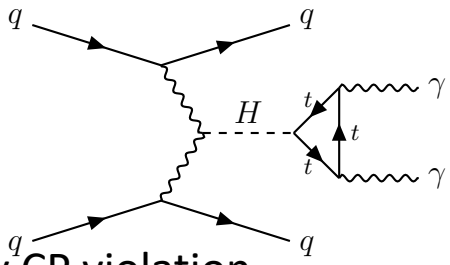

arXiv:2603.20087

Use of VBF production with clean $H \to \gamma\gamma$ final state to study CP violation

Multi-class neural network separates VBF H, ggF H, and continuum $\gamma\gamma$ background

Use of optimal observable (OO) for $c_{H\tilde{W}}$, other HVV coefficients SM

Run 3 gives 40% improvement compared to Run 2, with 30% from new NN-based classification

Run 2 + Run 3 combination gives 50% total improvement in constraint

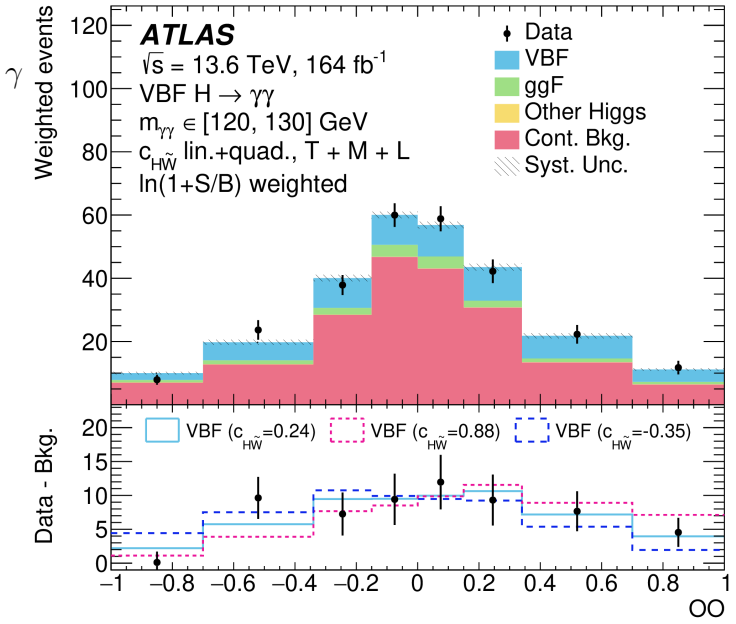

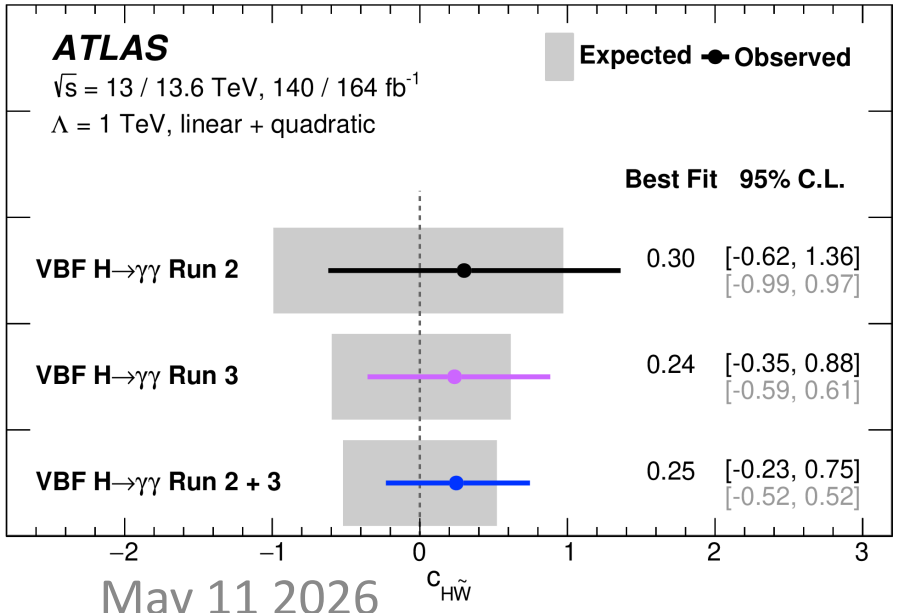

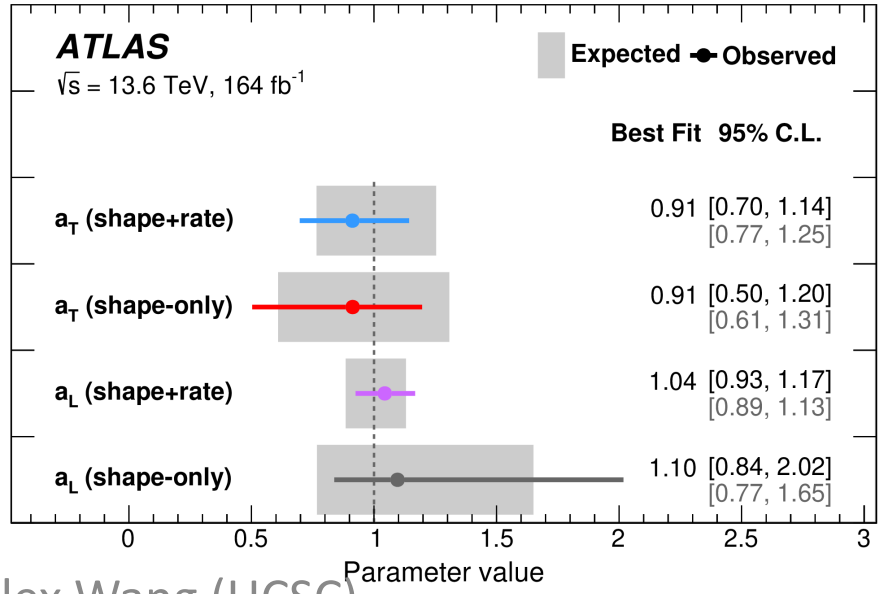

Longitudinal/transverse polarization HVV couplings also studied using $\Delta\phi_{jj}$ (first time in this channel)

$$a_{\mathrm{L}} = \frac{g_{HV_{\mathrm{L}}V_{\mathrm{L}}}}{g_{HVV}}, \quad a_{\mathrm{T}} = \frac{g_{HV_{\mathrm{T}}V_{\mathrm{T}}}}{g_{HVV}}$$

$HH \to bb\gamma\gamma$ EFT Run 2 + 3

Reinterpretation of $HH \to bb\gamma\gamma$ search*

Di-Higgs production allows unique probe into operators (e.g. c_H) not sensitive in single Higgs measurements

First interpretation accounting for EFT effects in VBF HH in addition to ggF HH

Higgs EFT results on $c_{hhh}, c_{gghh}, c_{tthh}$ also available

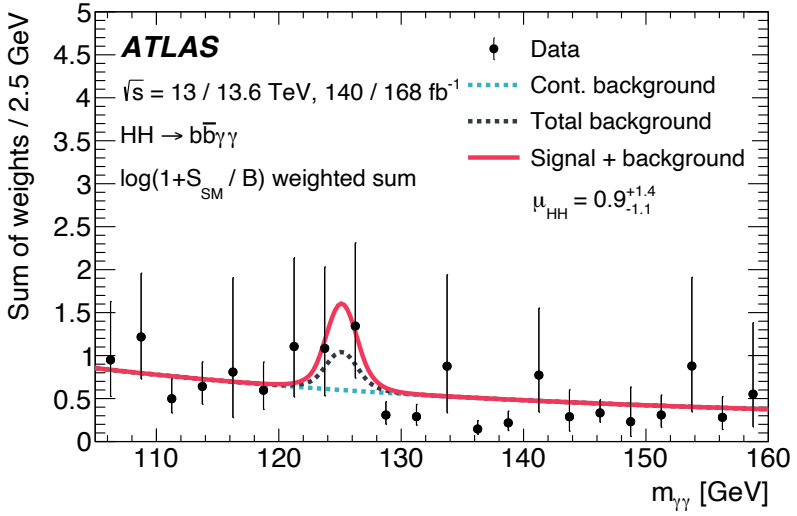

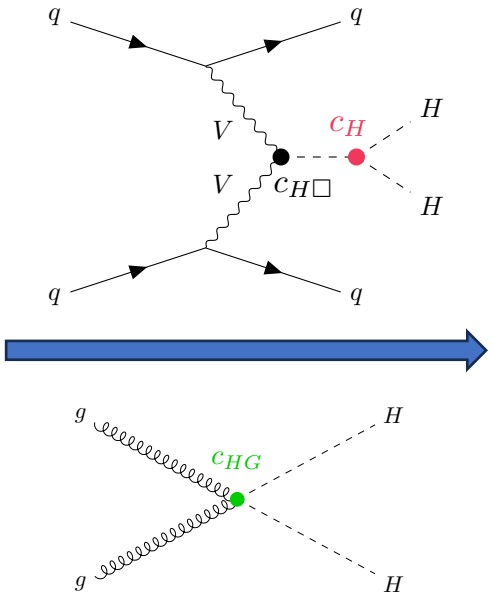

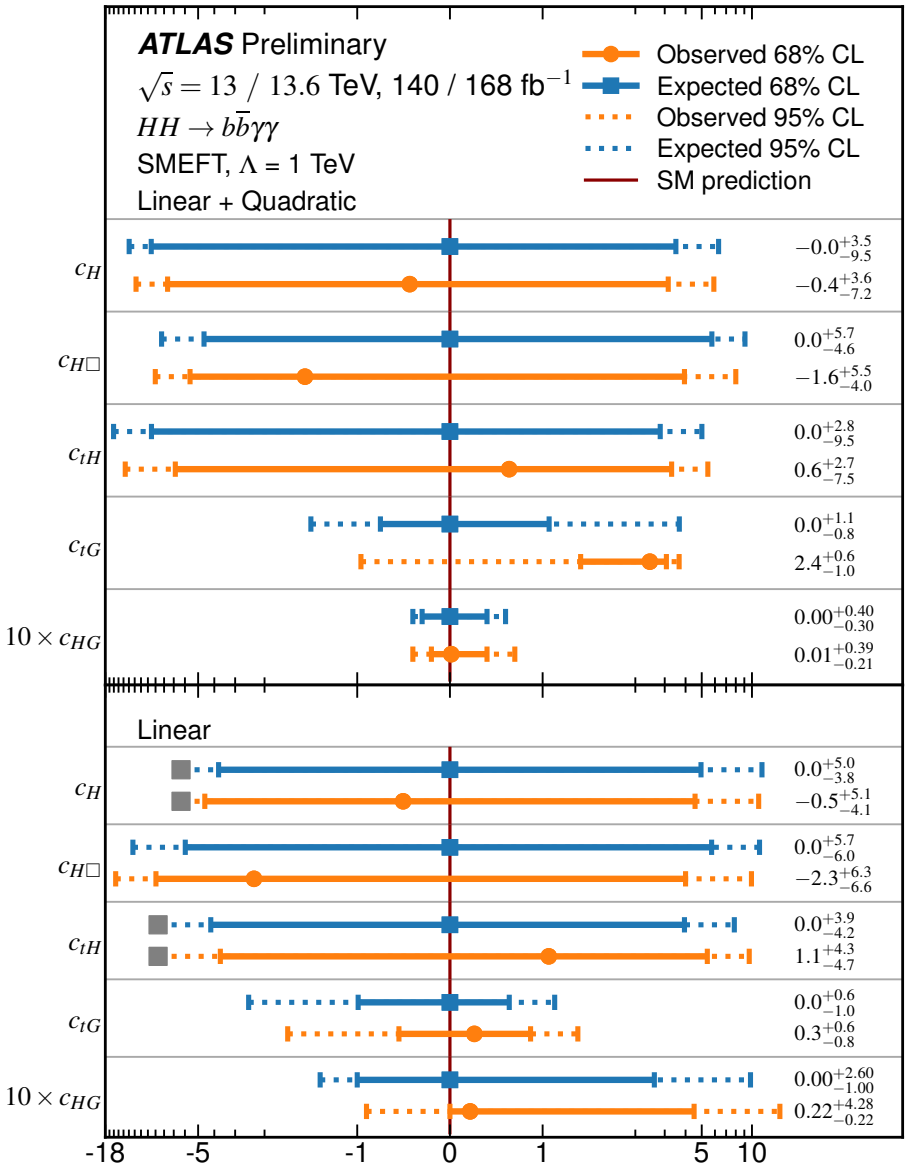

*See Romano's talk later today

~15% improvement compared to previous results

ATLAS Global EFT fit Run 2

arXiv:2604.21670

Most comprehensive EFT interpretation by ATLAS to date using Run 2 analyses as well as external electroweak precision observables

Total of 86 (CP even) Wilson coefficients, 47 simultaneously constrained using Principal Component Analysis

Re-interpretation in terms of 2 Higgs doublet models (2HDM) and Z' models also included

	Process
STXS	**Higgs boson measurements**
	$pp \to H \to \gamma\gamma,\ ZZ^* \to 4\ell,\ WW^* \to \ell\nu\ell\nu$
	$pp \to H \to Z\gamma,\ \mu^+\mu^-$
	$pp \to H \to b\bar{b},\ \tau^+\tau^-$
Differential x-sections	**Electroweak measurements**
	$pp \to W^+W^- \to e^\pm\nu\,\mu^\mp\nu$
	$pp \to W^\pm Z \to \ell^\pm\nu\,\ell^+\ell^-$
	$pp \to Zjj \to \ell^+\ell^- jj$
	HMDY measurements
	$pp \to Z/\gamma^* \to \tau^+\tau^-$
	$pp \to W^\pm \to \ell^\pm\nu$
	Top-quark measurements
	$pp \to t\bar{t} \to Wb\,Wb \to e^\pm\mu^\mp\nu\nu bb$
	$pp \to t\bar{t} \to Wb\,Wb \to qq'b\,\ell\nu b$
Inclusive x-sections, m_{HH}	**Di-Higgs measurements**
	$pp \to HH \to b\bar{b}\gamma\gamma,\ b\bar{b}\tau^+\tau^-$
	Electroweak precision observables
	LEP, SLD, ATLAS EWPO

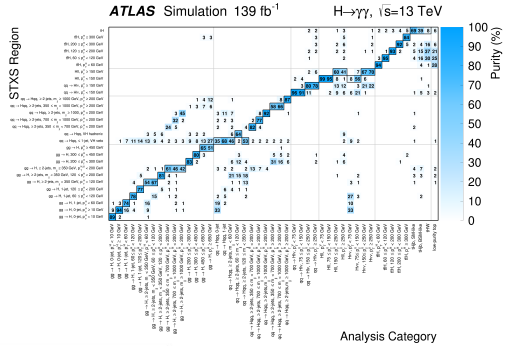

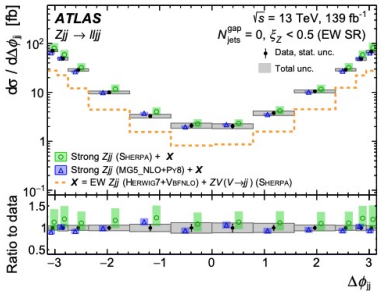

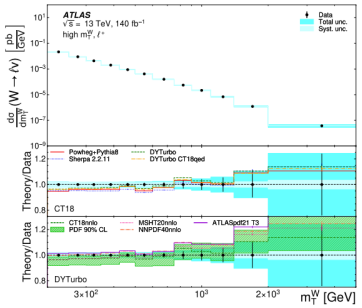

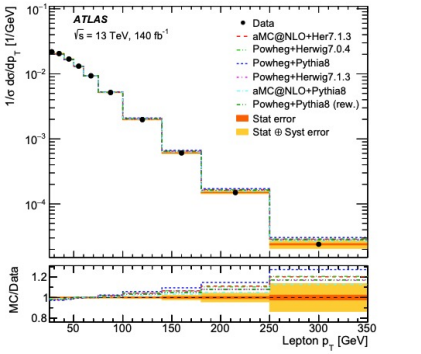

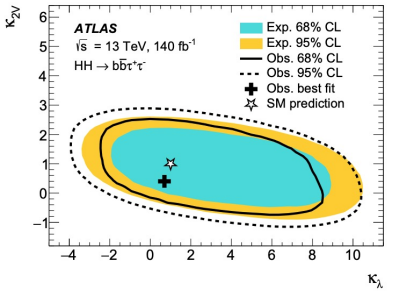

Observable	Measurement	Prediction	Ratio
$\Delta\alpha$	0.05903 ± 0.00009	0.05911 ± 0.00098	0.999 ± 0.017
Γ_Z [GeV]	2.4955 ± 0.0023	2.4945 ± 0.0010	1.0004 ± 0.0010
R_e	20.804 ± 0.050	20.751 ± 0.010	1.0025 ± 0.0024
R_μ	20.784 ± 0.034	20.751 ± 0.010	1.0016 ± 0.0017
R_τ	20.764 ± 0.045	20.799 ± 0.010	0.9983 ± 0.0022
R_c	0.1721 ± 0.0030	0.1722 ± 0.0001	0.999 ± 0.017
R_b	0.21629 ± 0.00066	0.21587 ± 0.00010	1.0019 ± 0.0031
σ^0_{had} [pb]	41481 ± 33	41489 ± 8	0.9998 ± 0.0008
A_e^{SLD}	0.1516 ± 0.0021	0.1470 ± 0.0025	1.031 ± 0.022
A_τ^{LEP}	0.1498 ± 0.0049	0.1470 ± 0.0025	1.019 ± 0.037
A_μ^{SLD}	0.142 ± 0.015	0.147 ± 0.003	0.97 ± 0.11
A_τ^{SLD}	0.136 ± 0.015	0.147 ± 0.003	0.92 ± 0.11
A_τ^{LEP}	0.1439 ± 0.0043	0.1470 ± 0.0025	0.979 ± 0.035
$A_{\text{FB}}^{0,e}$	0.0145 ± 0.0025	0.0162 ± 0.0006	0.89 ± 0.18
$A_{\text{FB}}^{0,\mu}$	0.0169 ± 0.0013	0.0162 ± 0.0006	1.042 ± 0.084
$A_{\text{FB}}^{0,\tau}$	0.0188 ± 0.0017	0.0162 ± 0.0006	1.159 ± 0.095
A_{FB}^{b}	0.0992 ± 0.0016	0.1031 ± 0.0018	0.962 ± 0.024
A_{FB}^{c}	0.0707 ± 0.0035	0.0737 ± 0.0014	0.959 ± 0.053
A_b	0.923 ± 0.020	0.935 ± < 0.001	0.987 ± 0.022
A_c	0.670 ± 0.027	0.668 ± 0.001	1.003 ± 0.040
Γ_W [GeV]	2.198 ± 0.049	2.090 ± 0.001	1.052 ± 0.022
B_W^e	0.1071 ± 0.0016	0.1082 ± < 0.0001	0.990 ± 0.015
B_W^μ	0.1063 ± 0.0015	0.1082 ± < 0.0001	0.983 ± 0.014
B_W^τ	0.1138 ± 0.0021	0.1082 ± < 0.0001	1.052 ± 0.018
$R_{WZ}^{\mu/e}$	0.9990 ± 0.0042	1.0000 ± < 0.0001	0.999 ± 0.004
$R_W^{\tau/\mu}$	0.992 ± 0.013	1.000 ± < 0.001	0.992 ± 0.013

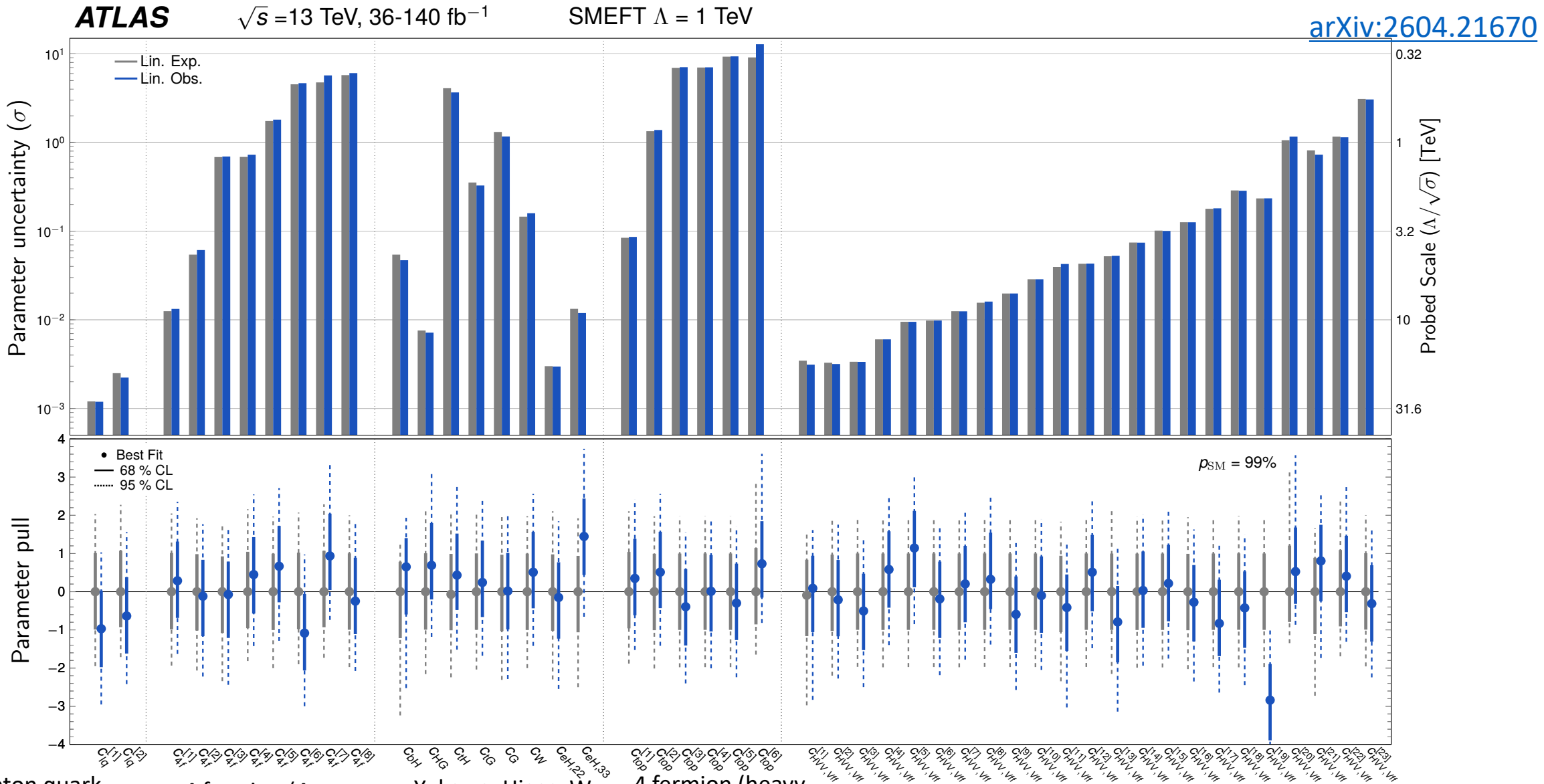

arXiv:2604.21670

Lepton quark interaction from charged current HMDY

4 fermion (4q, 2q2l) operators from HMDY / EW

Yukawa, Higgs, W and g self-couplings

4 fermion (heavy quark) operators from $t\bar{t}$

Electroweak precision observables, as well as $H \to \gamma\gamma$, $Z \to ll$, VH

In general consistent with SM within 2σ
Similar results for linear + quadratic fit

Summary

Today I showed you some of the latest results from ATLAS in understanding Higgs CP properties and EFT measurements

No concrete BSM evidence so far, but …

First set of Run 3 ATLAS constraints now becoming available with more luminosity, better analysis techniques

Stay tuned for more exciting results!

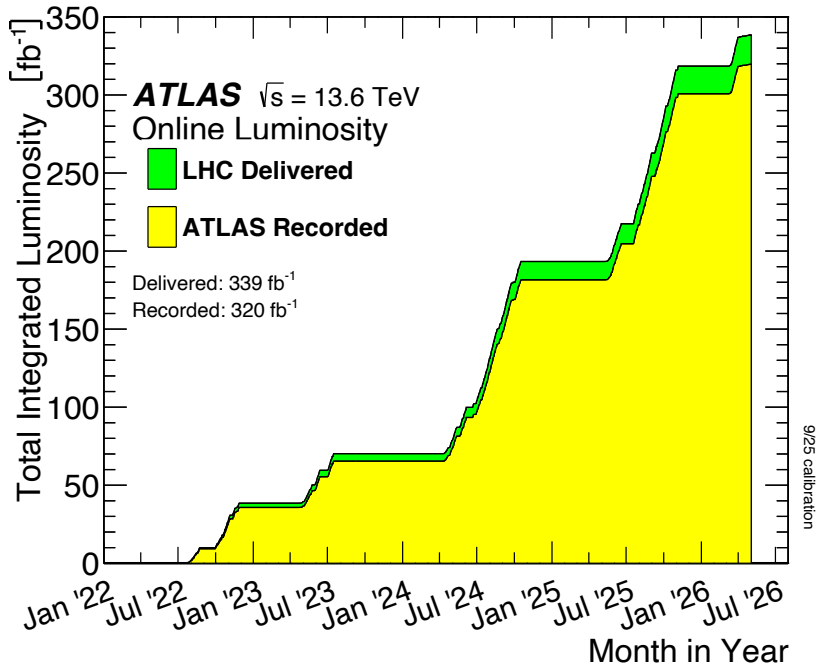

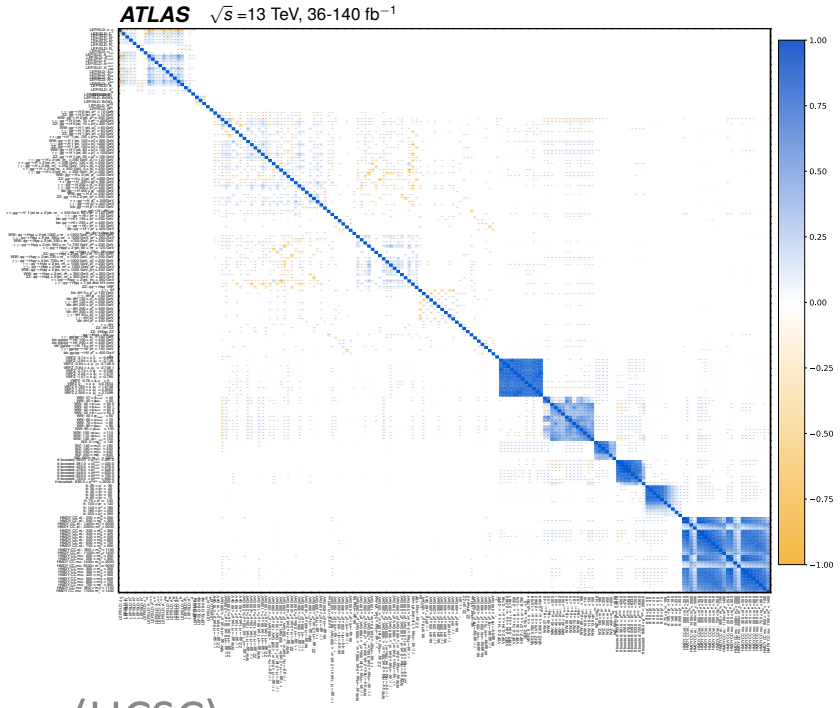

Correlation matrix from simultaneous signal strength fit in global EFT

Backup

VBF $H \rightarrow \tau\tau$ CP Run 2

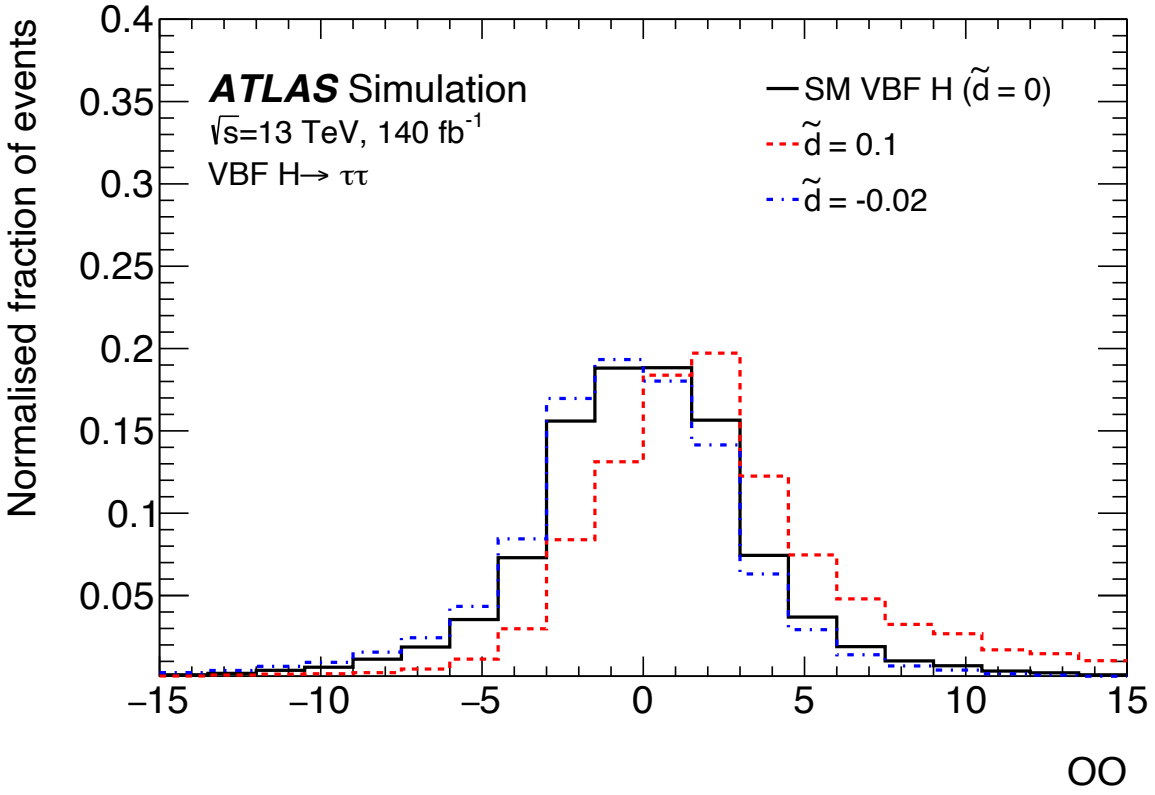

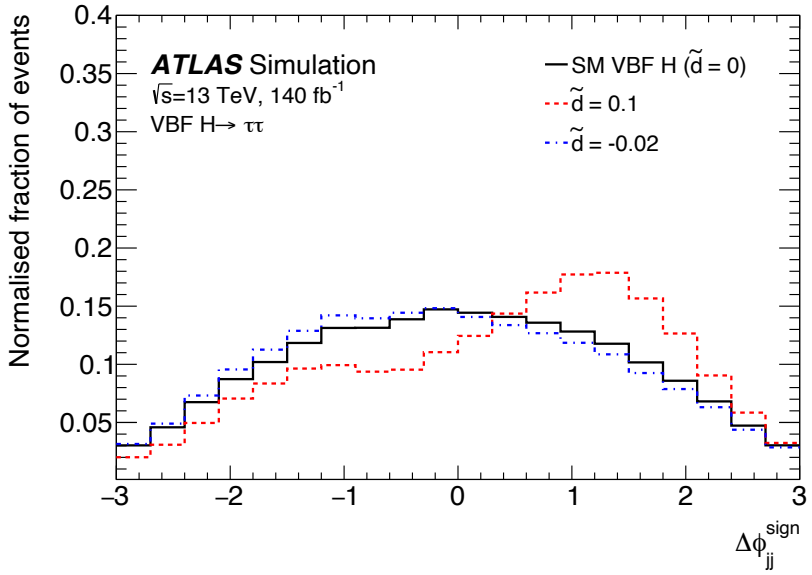

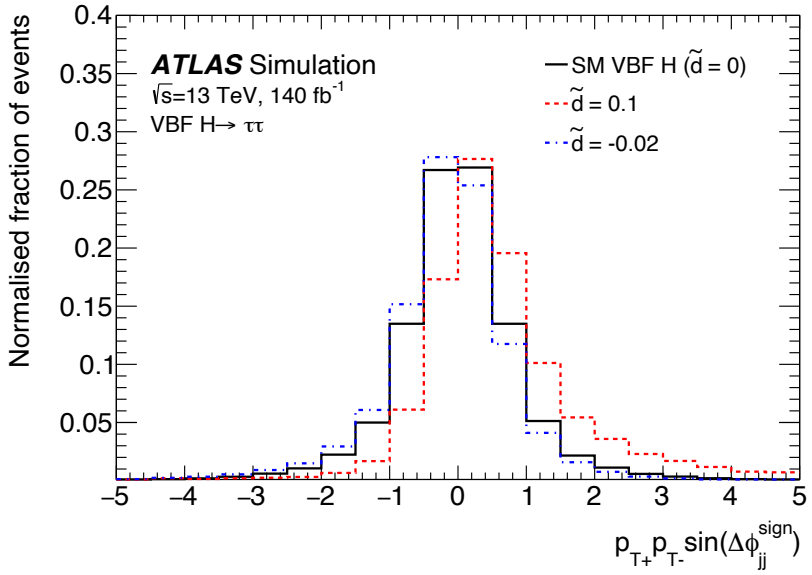

$HH \to bb\gamma\gamma$

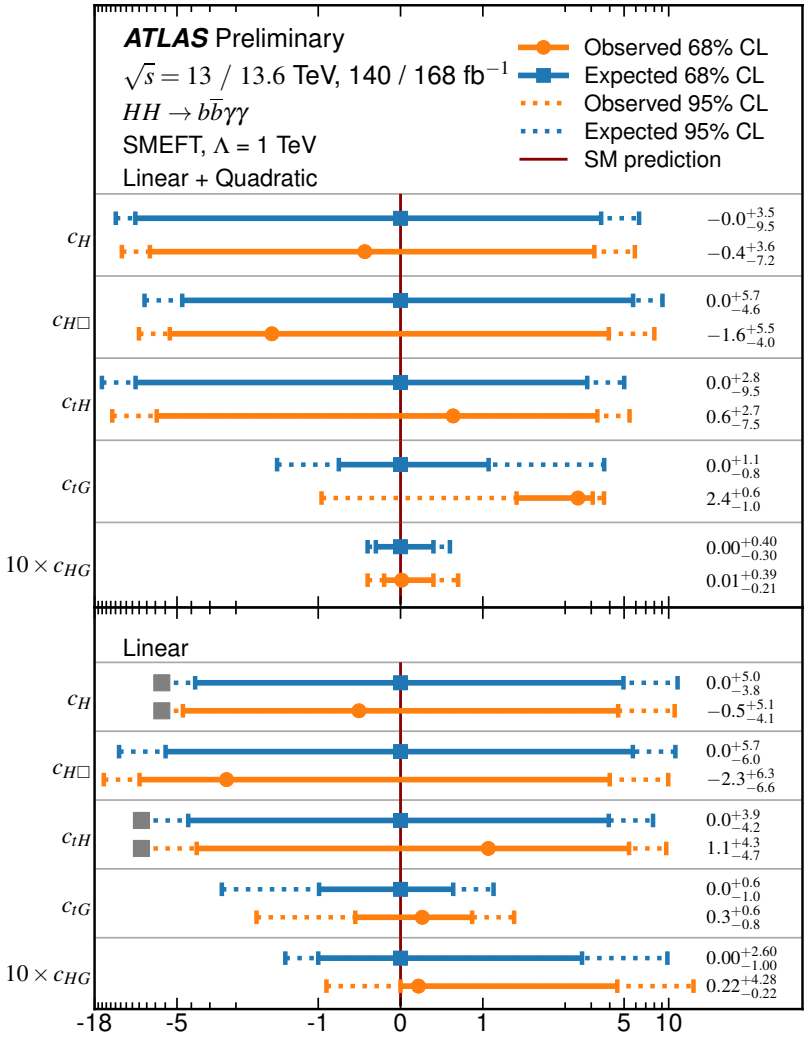

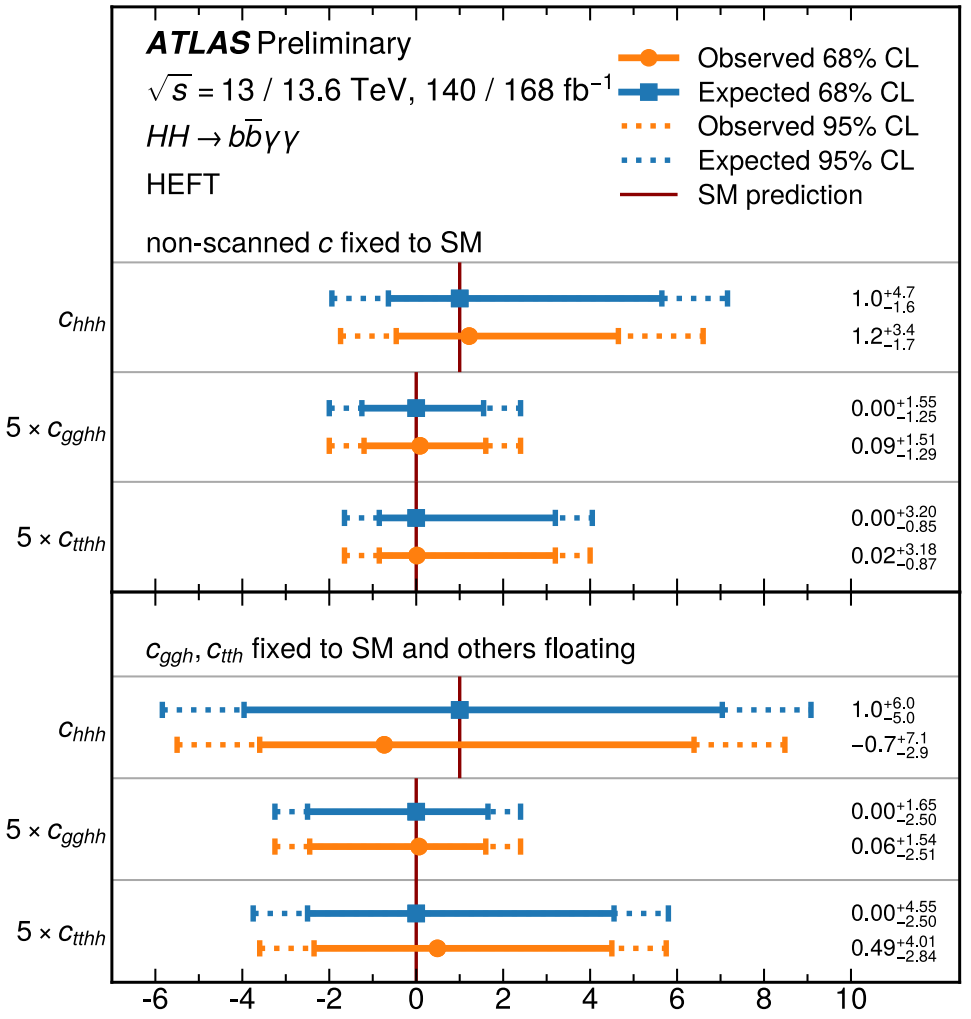

$HH \to bb\gamma\gamma$ SMEFT operators

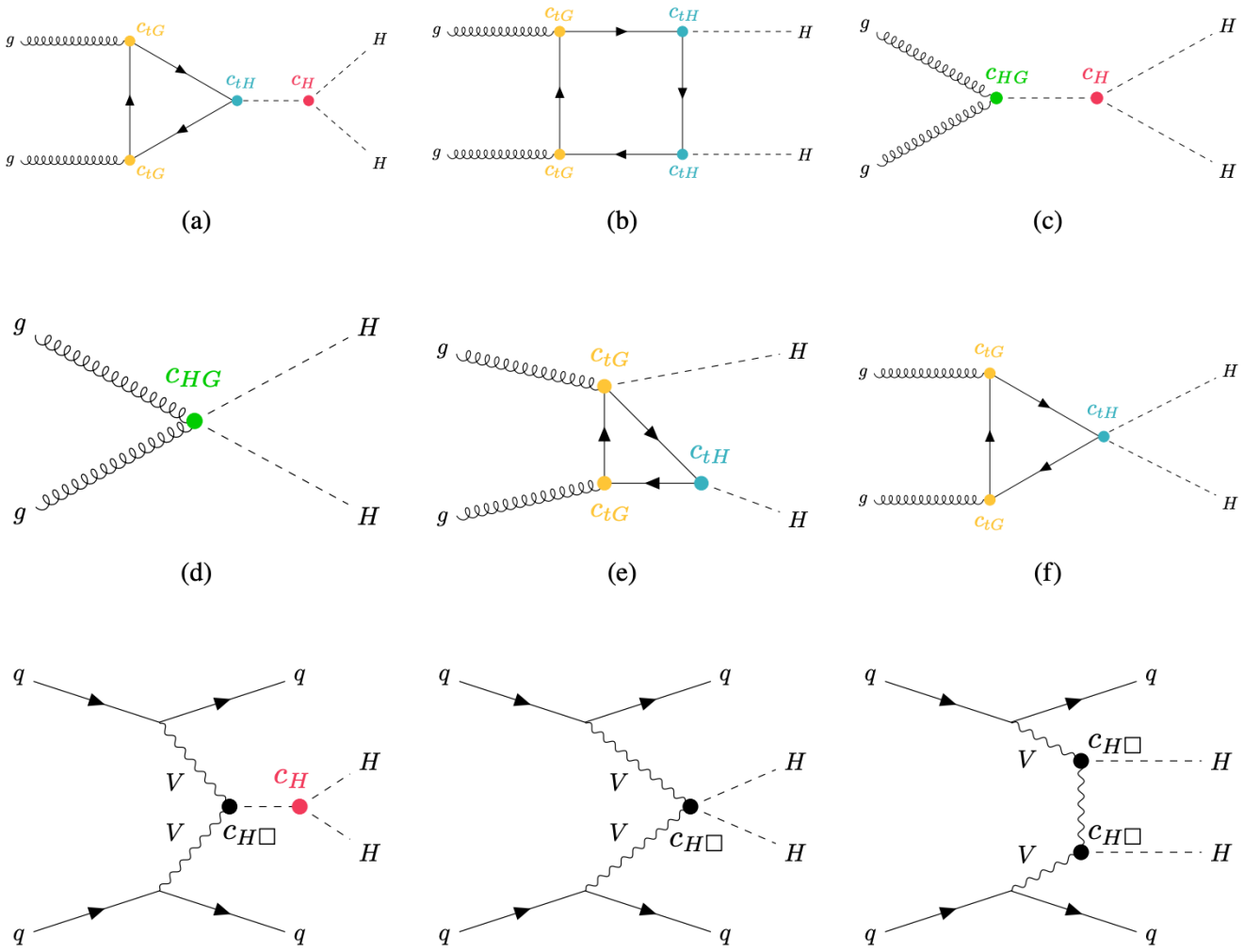

Five operators defined in the Warsaw basis [20] are considered in the SMEFT analysis that modify the Higgs self-coupling and ggF HH production cross section. The operator O_H uniquely modifies the Higgs self-coupling and is of primary interest in the SMEFT analysis. The operators $O_{H\Box}$ universally rescale all Higgs boson couplings. The operator O_{HG} generates three- and four-point interactions between the Higgs boson and gluons, while O_{tH} modifies the top-quark Yukawa interaction and generates a four-point interaction. These O_{HG} and O_{tH} operators also affect ggF and top-quark-associated single-Higgs production. The operator O_{tG} modifies the top-gluon interactions and adds a four-point interaction between top quarks, a Higgs boson, and a gluon. The operator $O_{H\Box}$ has a negligible effect on the branching fractions of the Higgs boson, while the effects of O_H enter only at NLO and are therefore neglected. The operators O_{HG} and O_{tG} modify the $H \to \gamma\gamma$ and $H \to b\bar{b}$ branching fractions through modifications on the $H \to gg$ partial width, while O_{tH} also directly modifies the $H \to \gamma\gamma$ partial width. Three operators are considered in the HEFT

$HH \to bb\gamma\gamma$ HEFT operators

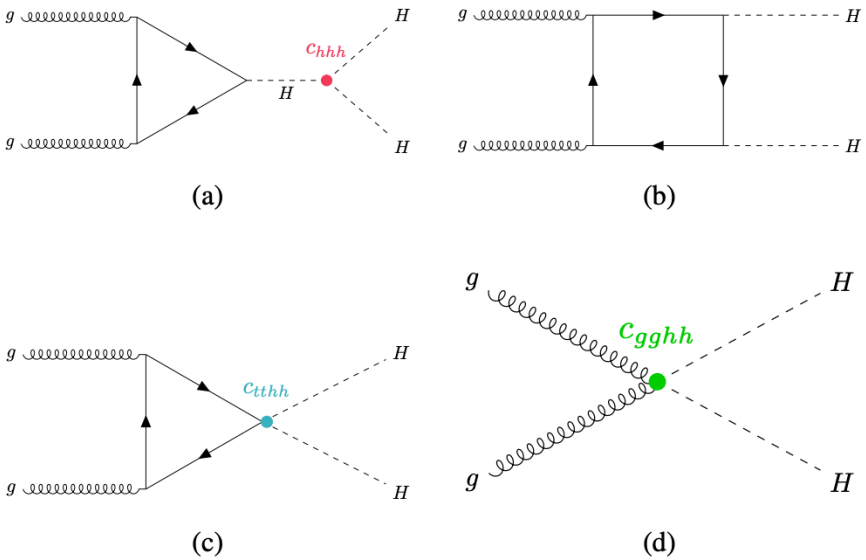

while O_{tH} also directly modifies the $H \to \gamma\gamma$ partial width. Three operators are considered in the HEFT analysis that modify interactions involving pairs of Higgs bosons that contribute primarily to ggF HH production. O_{hhh} modifies the Higgs self-coupling, O_{tthh} and O_{gghh} generate four-point interactions of pairs of Higgs bosons with top quarks or gluons, and O_{tth} modifies the top-quark Yukawa interaction. The

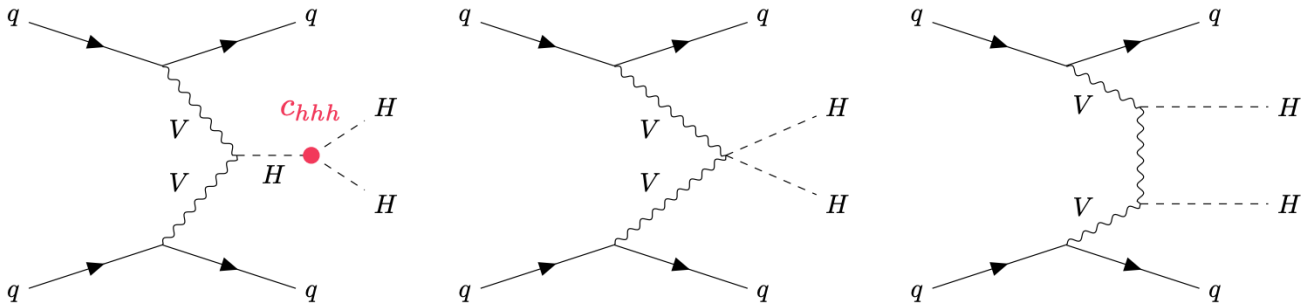

Global EFT inputs

The $\{m_W, m_Z, G_F\}$ electroweak input parameter scheme is used for the theoretical prediction of observables at the LHC and LEP. The measurements of the Z boson mass m_Z at LEP [29] and the W boson mass m_W at ATLAS [33] are sufficiently model-independent for these inputs to remain valid in a more general SMEFT scenario. The value of the Fermi constant G_F is determined from muon decays, which are affected by the Wilson coefficients $c^{(1)}_{Hl,33}$ and c_{ll}, such that the true value of G_F is a function of these parameters. Quarks from the first two generations and leptons from all three generations are assumed to be massless, and the four-flavour scheme is used for parton distribution functions. In this interpretation, the top-flavour symmetry scheme is adopted, which assumes a $U(2)^3$ symmetry in the quark sector. Under this scheme, the quarks of the first two generations and the third generation are treated independently. In the lepton sector, flavour diagonality is assumed, so that the lepton-antilepton pair of each generation is described independently. These relaxed assumptions allow for a dedicated treatment of heavy-flavour quarks and each lepton generation, enabling tests of lepton flavour universality violation.

Only operators that conserve charge-parity (CP) symmetry, i.e. CP-even operators, are considered and the Wilson coefficients are assumed to be real-valued. The list of operators and corresponding Wilson coefficients relevant to the processes studied in this paper is given in Table 8 and Table 9. The Warsaw basis operators are grouped into purely bosonic operators, operators containing both boson and fermion fields, four-lepton operators, four-fermion operators containing both quark and lepton fields, and four-quark operators. Operators with negligible impact on the combined measurements within the sensitivity of the datasets considered are not included in these tables.

Global EFT inputs

Process	Dataset [fb^{-1}]	SMEFT sensitivity
Higgs boson measurements		
$pp \to H \to \gamma\gamma,\ ZZ^* \to 4\ell,\ WW^* \to \ell\nu\ell\nu$	140	Higgs boson operators
$pp \to H \to Z\gamma,\ \mu^+\mu^-$	140	Higgs boson operators
$pp \to H \to b\bar{b},\ \tau^+\tau^-$	126–140	Higgs boson operators
Electroweak measurements		
$pp \to W^+W^- \to e^\pm\nu\,\mu^\mp\nu$	36	four-fermion operators and triple gauge couplings
$pp \to W^\pm Z \to \ell^\pm\nu\,\ell^+\ell^-$	36	four-fermion operators and triple gauge couplings
$pp \to Zjj \to \ell^+\ell^- jj$	140	four-fermion operators and triple gauge couplings
HMDY measurements		
$pp \to Z/\gamma^* \to \tau^+\tau^-$	140	four-fermion operators involving leptons
$pp \to W^\pm \to \ell^\pm\nu$	140	four-fermion operators involving leptons
Top-quark measurements		
$pp \to t\bar{t} \to Wb\,Wb \to e^\pm\mu^\mp\nu\nu bb$	140	four-fermion (heavy-flavour) operators
$pp \to t\bar{t} \to Wb\,Wb \to qq'b\,\ell\nu b$	140	four-fermion (heavy-flavour) operators
Di-Higgs measurements		
$pp \to HH \to b\bar{b}\gamma\gamma,\ b\bar{b}\tau^+\tau^-$	140	trilinear Higgs boson self-coupling
Electroweak precision observables		
LEP, SLD, ATLAS EWPO	–	Weak boson–fermion couplings

Decay channel	Production mode	$\mathcal{L}$ [fb^{-1}]	Ref.
$H \to \gamma\gamma$	ggF, VBF, WH, ZH, $t\bar{t}H$, tH	140	
$H \to ZZ^*$	ggF, VBF, WH + ZH, $t\bar{t}H$ + tH	140	
$H \to \tau\tau$	ggF, VBF, WH + ZH, $t\bar{t}H$ + tH	140	
$H \to WW^*$	ggF, VBF	140	
$H \to b\bar{b}$	WH, ZH	140	
	VBF	126	
	$t\bar{t}H$ + tH	140	
	inclusive	140	
$H \to Z\gamma$	inclusive	140	
$H \to \mu\mu$	ggF + $t\bar{t}H$ + tH, VBF + WH + ZH	140	

Process	Main phase-space requirements	Observable	$\mathcal{L}$ [fb^{-1}]	Ref.
$pp \to W^+W^- \to e^\pm\nu\,\mu^\mp\nu$	$m_{\ell\ell} > 55$ GeV, $p_{\mathrm{T}}^{\mathrm{jet}} > 35$ GeV	p_{T}^{ℓ}	36	
$pp \to W^\pm Z \to \ell^\pm\nu\,\ell^+\ell^-$	$m_{\ell\ell} \in (66, 116)$ GeV, $m_{\mathrm{T}}^{W} > 30$ GeV	m_{T}^{WZ}	36	
$pp \to Zjj \to \ell^+\ell^- jj$	$m_{jj} > 1000$ GeV, $m_{\ell\ell} \in (81, 101)$ GeV	$\Delta\phi_{jj}$	140	

Process	Important phase-space requirements	Observable	$\mathcal{L}$ [fb^{-1}]	Ref.
$pp \to Z/\gamma^* \to \tau^\pm\tau^\mp$	$m_{\tau\tau}^{vis} > 100$ GeV	$m_{\tau\tau}^{vis}$	140	
$pp \to W \to \ell^\pm\nu$ (with $\ell = e, \mu$)	$200 < m_{\mathrm{T}}^{W} < 5000$ GeV	m_{T}^{W}	140	

Process	Important phase-space requirements	Observable	$\mathcal{L}$ [fb^{-1}]	Ref.
$pp \to t\bar{t} \to Wb\,Wb \to e^\pm\mu^\mp\nu\nu bb$	p_{T}^{ℓ} >27 GeV, $\lvert\eta(\ell)\rvert < 2.5$	p_{T}^{ℓ}	140	
$pp \to t\bar{t} \to Wb\,Wb \to qq'b\,\ell\nu b$	$p_{\mathrm{T}}^{J} > 355$ GeV	$p_{\mathrm{T}}^{t,h}$	140	

Process	Production mode	$\mathcal{L}$ [fb^{-1}]	Ref.
$HH \to b\bar{b}\gamma\gamma$	ggF	140	
$HH \to b\bar{b}\tau\tau$	ggF	140	

Global EFT inputs

Observable	Measurement	Prediction	Ratio
$\Delta\alpha$	0.05903 ± 0.00009	0.05911 ± 0.00098	0.999 ± 0.017
Γ_Z [GeV]	2.4955 ± 0.0023	2.4945 ± 0.0010	1.0004 ± 0.0010
R_e	20.804 ± 0.050	20.751 ± 0.010	1.0025 ± 0.0024
R_μ	20.784 ± 0.034	20.751 ± 0.010	1.0016 ± 0.0017
R_τ	20.764 ± 0.045	20.799 ± 0.010	0.9983 ± 0.0022
R_c	0.1721 ± 0.0030	0.1722 ± 0.0001	0.999 ± 0.017
R_b	0.21629 ± 0.00066	0.21587 ± 0.00010	1.0019 ± 0.0031
σ^0_{had} [pb]	41481 ± 33	41489 ± 8	0.9998 ± 0.0008
A_e^{SLD}	0.1516 ± 0.0021	0.1470 ± 0.0025	1.031 ± 0.022
A_e^{LEP}	0.1498 ± 0.0049	0.1470 ± 0.0025	1.019 ± 0.037
A_μ^{SLD}	0.142 ± 0.015	0.147 ± 0.003	0.97 ± 0.11
A_τ^{SLD}	0.136 ± 0.015	0.147 ± 0.003	0.92 ± 0.11
A_τ^{LEP}	0.1439 ± 0.0043	0.1470 ± 0.0025	0.979 ± 0.035
$A_{\text{FB}}^{0,e}$	0.0145 ± 0.0025	0.0162 ± 0.0006	0.89 ± 0.18
$A_{\text{FB}}^{0,\mu}$	0.0169 ± 0.0013	0.0162 ± 0.0006	1.042 ± 0.084
$A_{\text{FB}}^{0,\tau}$	0.0188 ± 0.0017	0.0162 ± 0.0006	1.159 ± 0.095
$A_{\text{FB}}^{0,b}$	0.0992 ± 0.0016	0.1031 ± 0.0018	0.962 ± 0.024
$A_{\text{FB}}^{0,c}$	0.0707 ± 0.0035	0.0737 ± 0.0014	0.959 ± 0.053
A_b	0.923 ± 0.020	0.935 ± < 0.001	0.987 ± 0.022
A_c	0.670 ± 0.027	0.668 ± 0.001	1.003 ± 0.040
Γ_W [GeV]	2.198 ± 0.049	2.090 ± 0.001	1.052 ± 0.022
B_W^e	0.1071 ± 0.0016	0.1082 ± < 0.0001	0.990 ± 0.015
B_W^μ	0.1063 ± 0.0015	0.1082 ± < 0.0001	0.983 ± 0.014
B_W^τ	0.1138 ± 0.0021	0.1082 ± < 0.0001	1.052 ± 0.018
$R_{WZ}^{\mu/e}$	0.9990 ± 0.0042	1.0000 ± < 0.0001	0.999 ± 0.004
$R_W^{\tau/\mu}$	0.992 ± 0.013	1.000 ± < 0.001	0.992 ± 0.013

2.6 Electroweak precision observables

The EWPO considered in this analysis probe the couplings of the Z and W bosons to charged leptons, neutrinos, and heavy quarks. Key observables measured at LEP and SLD [29] include the total and partial Z widths, Γ_Z, the hadronic cross-section at the Z pole (defined as the total cross-section for Z decays into hadrons), σ_{had}, the ratio of hadronic to leptonic Z-boson decays for charged leptons, R_ℓ, and the fractions of hadronic Z decays into charm and bottom quarks, R_c and R_b, respectively. Forward–backward asymmetries $A_{\text{FB}}^{0,f}$, lepton polarisation and asymmetry measurements, W-boson branching ratios are also included.

Additionally, ATLAS measurements of lepton-flavour-universality ratios [30–32], $R_W^{\tau/\mu}$ and $R_{WZ}^{\mu/e}$, and the W-boson total width [33] are considered. These observables provide sensitivity to deviations from the SM through their dependence on left- and right-handed electroweak couplings.

Table 7: Electroweak precision observables [29–33], included in the analysis. The second column corresponds to the experimental value, the third to the theory prediction in the $\{m_W, m_Z, G_F\}$ scheme, and the fourth is the ratio of the two values. The correlation between the observables is shown in Table 10.

PCA decomposition

$$
\begin{aligned}
\boldsymbol{c} = {} & \{c_{eH,22}\} \cup \\
& \{c_{eH,33}\} \cup \\
& \{c_{G}\} \cup \\
& \{c_{HG}\} \cup \\
& \{c_{tG}\} \cup \\
& \{c_{tH}\} \cup \\
& \{c_{bH}\} \cup \\
& \{c_{W}\} \cup \\
& \{c_{lq,11}{}^{(3)}, c_{lq,22}{}^{(3)}\} \cup \\
& \{c_{td}^{(1)}, c_{Qd}^{(1)}, c_{Qd}^{(8)}, c_{Qq}^{(1,1)}, c_{Qq}^{(1,8)}, c_{Qq}^{(3,1)}, c_{Qq}^{(3,8)}, c_{Qu}^{(1)}, c_{Qu}^{(8)}, c_{td}^{(8)}, c_{tq}^{(1)}, \\
& c_{tq}^{(8)}, c_{tu}^{(1)}, c_{tu}^{(8)}, c_{qq}^{(1,1)}, c_{qq}^{(1,8)}, c_{qq}^{(3,1)}, c_{qq}^{(3,8)}, c_{uu}^{(1)}, c_{qu}^{(8)}, c_{qd}^{(8)}\} \cup \\
& \{c_{Qe,22}, c_{Ql,22}{}^{(1)}, c_{Ql,22}{}^{(3)}, c_{be,22}, c_{bl,22}, c_{ed,22}, c_{eu,22}, c_{ej,22}, c_{ld,22}, \\
& c_{lu,22}, c_{lq,22}{}^{(3)}, c_{Qe,33}, c_{Ql,33}{}^{(3)}, c_{Ql,33}{}^{(1)}, c_{be,11}, c_{bl,11}, c_{ed,11}, \\
& c_{eu,11}, c_{ej,11}, c_{lq,11}{}^{(1)}, c_{lq,22}{}^{(1)}, c_{lq,11}{}^{(3)}, c_{lu,11}, c_{ld,11}\} \cup \\
& \{c_{HDD}, c_{HQ}^{(1)}, c_{HQ}^{(3)}, c_{Hb}, c_{Hd}, c_{He,11}, \\
& c_{Hq}^{(3)}, c_{Hl,11}^{(1)}, c_{Hl,22}^{(1)}, c_{Hl,33}^{(1)}, c_{Hl,11}^{(3)}, c_{Hl,22}^{(3)}, c_{Hl,33}^{(3)}, \\
& c_{HB}, c_{HW}, c_{HWB}, c_{H\Box}, \\
& c_{bB}, c_{bW}, c_{He,22}, c_{He,33}, c_{Hq}^{(1)}, \\
& c_{eW}^{33}, c_{eB}^{33}, c_{tB}, \\
& c_{Hl,33}^{(3)}, c_{Hu}, c_{ll,1221}\}
\end{aligned}
$$

$$
\begin{aligned}
\boldsymbol{c}' = {} & \{c_{eH,22}\} \cup \\
& \{c_{eH,33}\} \cup \\
& \{c_{G}\} \cup \\
& \{c_{HG}\} \cup \\
& \{c_{tG}\} \cup \\
& \{c_{tH}\} \cup \\
& \{c_{bH}\} \cup \\
& \{c_{W}\} \cup \\
& \{c_{lq}^{[1]}, c_{lq}^{[2]}\} \cup \\
& \{c_{\text{top}}^{[1]}, c_{\text{top}}^{[2]}, c_{\text{top}}^{[3]}, \\
& c_{\text{top}}^{[4]}, c_{\text{top}}^{[5]}, c_{\text{top}}^{[6]}, \} \cup \\
& \{c_{\text{4f}}^{[1]}, c_{\text{4f}}^{[2]}, c_{\text{4f}}^{[3]}, \\
& \{c_{\text{4f}}^{[4]}, c_{\text{4f}}^{[5]}, c_{\text{4f}}^{[6]}, \\
& c_{\text{4f}}^{[7]}, c_{\text{4f}}^{[8]}\} \cup \\
& \{c_{HVV,Vff}^{[1]}, c_{HVV,Vff}^{[2]}, c_{HVV,Vff}^{[3]}, c_{HVV,Vff}^{[4]}, \\
& c_{HVV,Vff}^{[5]}, c_{HVV,Vff}^{[6]}, c_{HVV,Vff}^{[7]}, c_{HVV,Vff}^{[8]}, \\
& c_{HVV,Vff}^{[9]}, c_{HVV,Vff}^{[10]}, c_{HVV,Vff}^{[11]}, c_{HVV,Vff}^{[12]}, \\
& c_{HVV,Vff}^{[13]}, c_{HVV,Vff}^{[14]}, c_{HVV,Vff}^{[15]}, c_{HVV,Vff}^{[16]}, \\
& c_{HVV,Vff}^{[17]}, c_{HVV,Vff}^{[18]}, c_{HVV,Vff}^{[19]}, c_{HVV,Vff}^{[20]}, \\
& c_{HVV,Vff}^{[21]}, c_{HVV,Vff}^{[22]}, c_{HVV,Vff}^{[23]}\}
\end{aligned}
$$

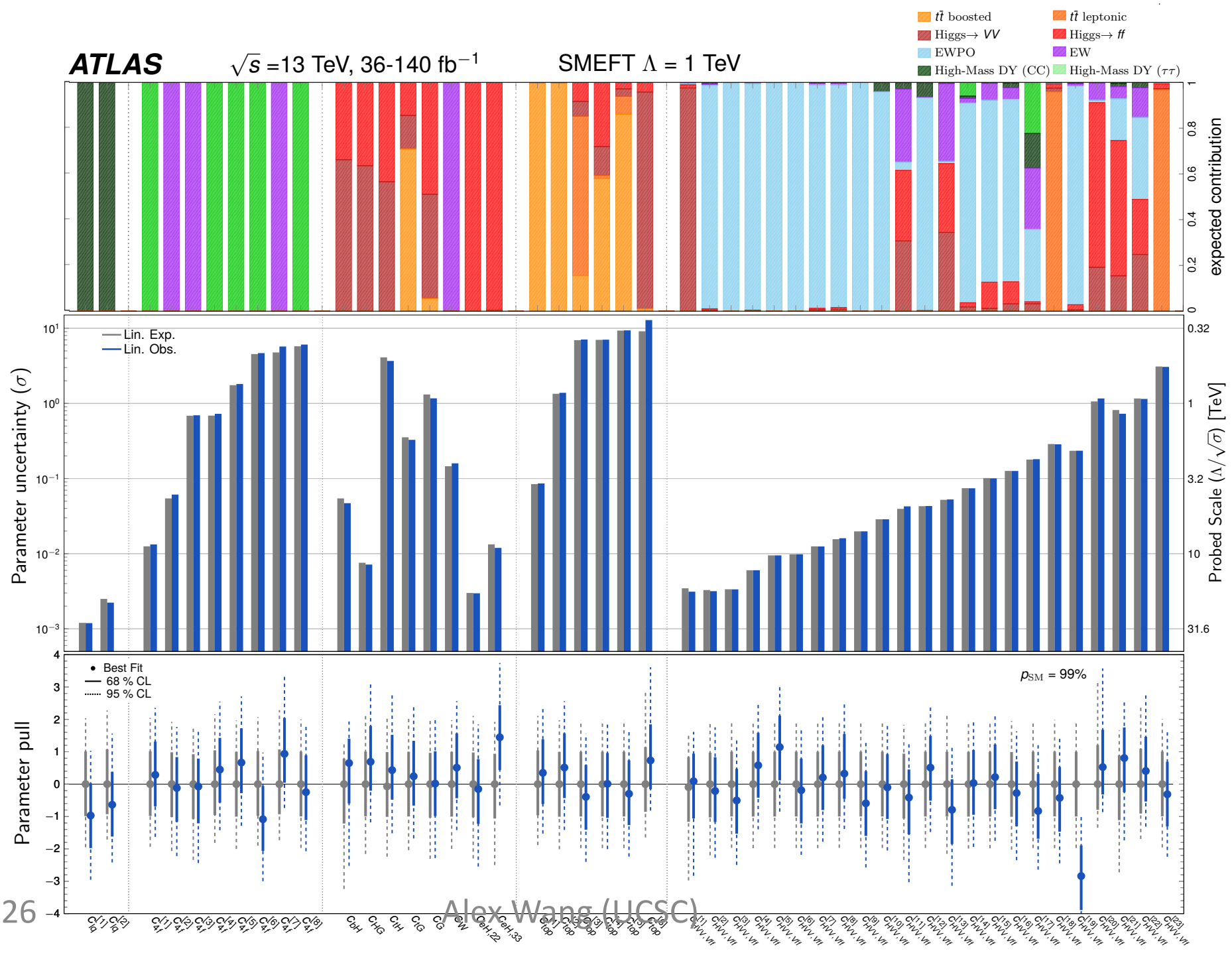
ATLAS
$\sqrt{s}$ =13 TeV, 36-140 fb^{-1}
SMEFT Λ = 1 TeV
$t\bar{t}$ boosted
$t\bar{t}$ leptonic
Higgs→ VV
Higgs→ ff
EWPO
EW
High-Mass DY (CC)
High-Mass DY ($\tau\tau$)
expected contribution
Lin. Exp.
Lin. Obs.
Parameter uncertainty (σ)
Probed Scale ($\Lambda/\sqrt{\sigma}$) [TeV]
Best Fit
68 % CL
95 % CL
p_{SM} = 99%
Parameter pull

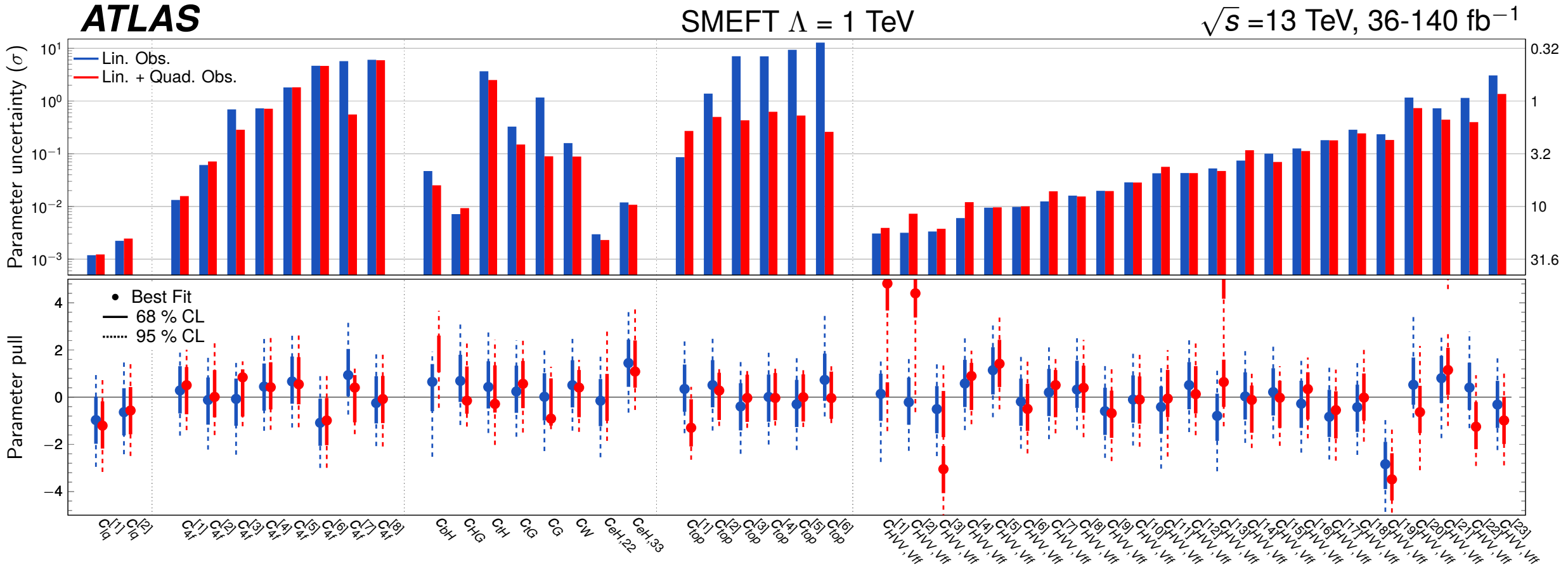

No significant deviation from the SM is observed: all coefficients are compatible with the SM expectation within 2σ. The only exception is $c^{[19]}_{HVV,Vff}$, constrained by EWPO and pulled by the well-known discrepancy between the $A^{0,b}_{FB}$ and $A^{0,c}_{FB}$ measurements and the SM expectations [113]. Good agreement between the observed data and the SM expectations is found, corresponding to a p-value of 99%.

Global EFT inputs

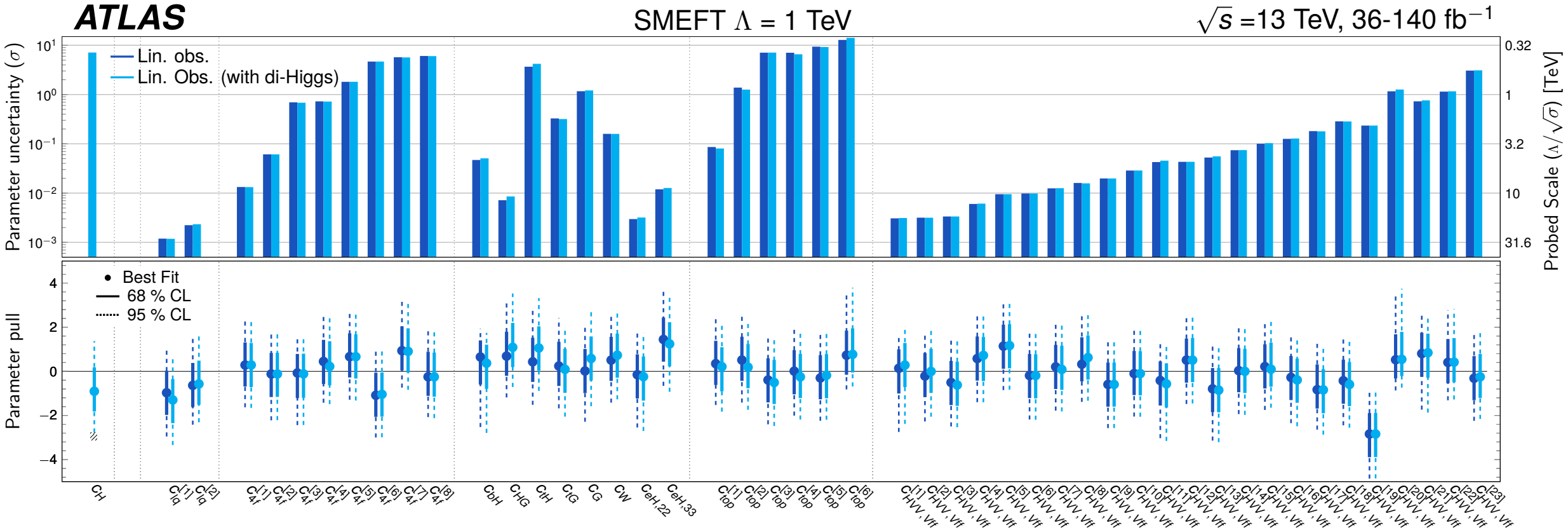

ATLAS Global EFT fit Run 2

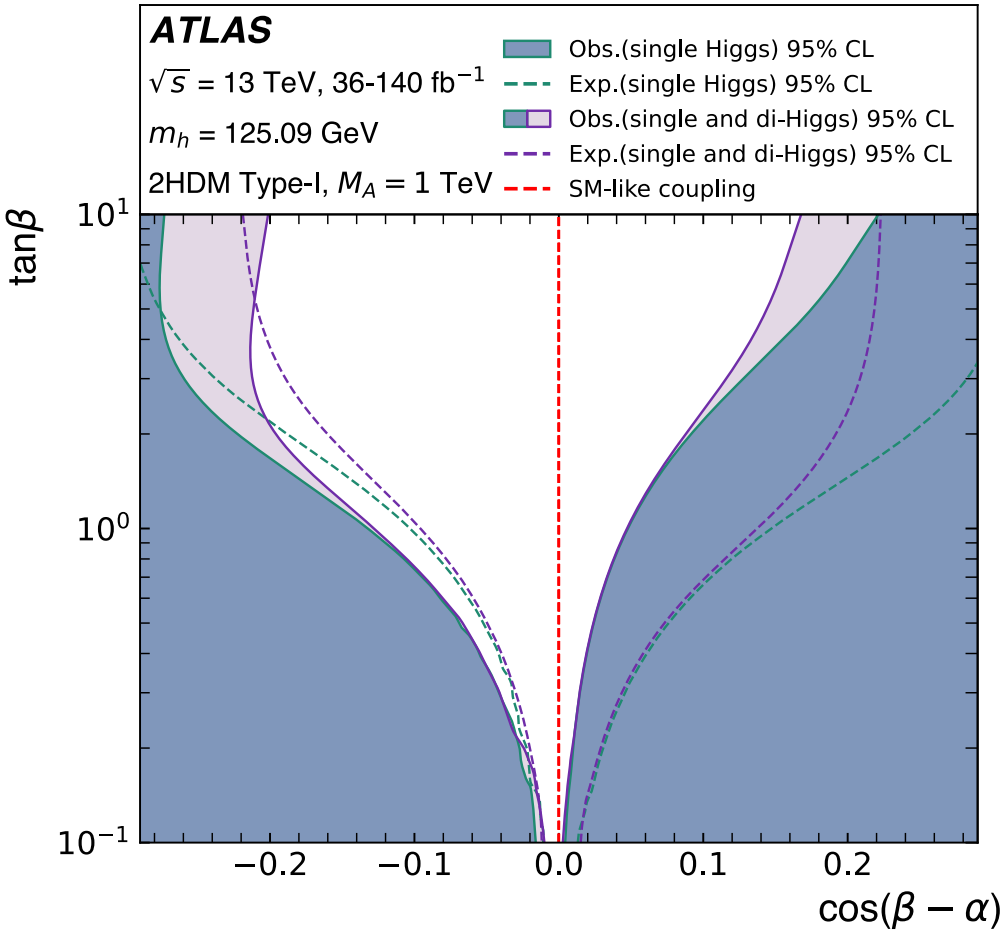

Re-interpretation in terms of 2 Higgs doublet models (2HDM) and Z' models also included

Relevant SMEFT coefficients mapped to 2HDM parameters via

$$\frac{v^2 c_H}{\Lambda^2} = \frac{\cos^2(\beta-\alpha) M_A^2}{v^2},$$
$$\frac{v^2 c_{bH}}{\Lambda^2} = -y_b \frac{\cos(\beta-\alpha)}{\tan\beta},$$
$$\frac{v^2 c_{tH}}{\Lambda^2} = -y_t \frac{\cos(\beta-\alpha)}{\tan\beta},$$
$$\frac{v^2 c_{\tau H}}{\Lambda^2} = -y_\tau \frac{\cos(\beta-\alpha)}{\tan\beta},$$
$$\frac{v^2 c_{\mu H}}{\Lambda^2} = -y_\mu \frac{\cos(\beta-\alpha)}{\tan\beta},$$

where $y_i = \sqrt{2} m_i / v$ for $i = b, t, \tau, \mu$, and v is the SM vacuum expectation value.